

Gas Phase Basicities and Relative Proton Affinities of Compounds between Water and Ammonia from Pulsed Ion Cyclotron Resonance Thermal Equilibria Measurements^{1a}

J. F. Wolf, R. H. Staley, I. Koppel,^{1b} M. Taagepera, R. T. McIver, Jr., J. L. Beauchamp,^{1c} and R. W. Taft*

Contribution from the Department of Chemistry, University of California, Irvine, California 92717, and the Arthur Amos Noyes Laboratory of Chemical Physics, California Institute of Technology, Pasadena, California 91125 (Contribution No. 5454). Received October 26, 1976

Abstract: The pulsed ion cyclotron resonance method for precise determinations of proton transfer equilibrium constants has been applied to 46 carbon, nitrogen, oxygen, phosphorus, sulfur, arsenic, and selenium bases, with duplicating overlapping sequences, to obtain the relative proton affinities of water and ammonia. Where comparison is possible, the results are in generally good accord with those obtained by high-pressure mass spectroscopy. The results provide important new insights into the intrinsic effects of molecular structure on base strengths. Applications of these results to derive other gaseous ion thermochemical data are illustrated. In particular, methyl substituent effects on proton affinities have been extensively evaluated and interpretations are made of the comparisons with corresponding effects on homolytic bond dissociation energies of the conjugate acids of *n*-bases and with the hydride affinities of substituted methyl cations. Comparisons of the effects of *n*-alkyl substituents on the proton affinities of water and alcohols with carboxylic acids and their esters indicate that protonation is thermodynamically favored in the gas phase at the carbonyl oxygen of the latter. Large effects of polar electronegative substituents have been observed for various oxygen and nitrogen bases. An evaluation of entropy effects in gas phase proton transfer equilibria shows such effects to be generally small for simple bases and approximately equal to entropy effects expected for changes in molecular rotational symmetry numbers. Finally, the present result provides the basis for evaluations of absolute proton affinities and of relative ion solvation energies.

The proton affinities (PA) of water and ammonia are fundamental to many interests in chemistry and biology. However, even the relative proton affinity of these substances has remained in substantial uncertainty. In 1932, Sherman² obtained from thermochemical data and lattice energy assumptions the estimate $PA(\text{NH}_3) - PA(\text{H}_2\text{O}) = 25 \text{ kcal mol}^{-1}$. Haney and Franklin³ obtained more recently the estimate of 41 kcal mol^{-1} for this difference in proton affinity, after attempting a correction for excess energies of ions formed by electron impact. While this work was in progress, Yamdagni and Kebarle⁴ reported $\Delta PA = 31.8 \pm 1-2 \text{ kcal mol}^{-1}$. Their value is based upon high-pressure mass spectrometric proton transfer equilibrium constant determinations.

In this study, we have applied the relatively precise determination of proton transfer equilibrium constants at 300 K by the pulsed ion cyclotron resonance (ICR) method⁵ to measuring stepwise, with duplicating overlapping sequences, the interval in gas phase base strengths between water and ammonia. The results serve eight important purposes: (1) a precise value for the PA of ammonia relative to water is obtained; (2) the validity of the equilibrium hypothesis for low-pressure ICR experiments is put to severe test; (3) a substantial body of new information is provided on the effects of molecular structure on base strengths toward the proton in the absence of solvent; (4) several applications are illustrated of the use of the relative PAs to evaluate other gaseous ion thermochemical data. For example, precise methyl substituent effects on proton affinities have been extensively evaluated and compared with the corresponding methyl substituent effects on the homolytic bond dissociation energies of the conjugate acids of *n*-bases, and on the hydride affinities of substituted methyl cations; (5) comparison of the standard free energy changes at 300 K obtained by the ICR method with the corresponding values at 600 K obtained by the high-pressure mass spectroscopic method⁴ offers general confirmation of both results; (6) an evaluation of the (small) role of entropy effects in gas phase proton transfer equilibria between simple bases has been made; (7)

with bases of known proton affinities, the accurate relative PAs give many new absolute values of PA;⁶ (8) in combination with solution thermodynamic quantities for proton transfer equilibria, the present results provide a means for precise quantitative evaluation of solvent effects and relative ion solvation energies.⁷

Experimental Section

Materials. Commercial samples of most compounds were utilized. All commercial samples were assayed for purity by mass spectrometry. If these samples were less than 99% pure, preparative gas chromatography was employed to obtain samples of this purity.

Methyl ethyl ether was prepared by reacting ethyl iodide with sodium methoxide and purified by vacuum line trap-to-trap distillation.

***n*-Butyl, *n*-propyl, and methyl trifluoroacetates** were prepared by reacting trifluoroacetic anhydride with the respective alcohol. Purification was effected by gas chromatography.

Formaldehyde was prepared by heating paraformaldehyde under vacuum and allowing the monomer to distill into an evacuated bulb.

HCN was prepared by reacting NaCN with H₂SO₄. Purification was effected by vacuum line trap-to-trap distillation.

CF₃CO₂(CH₂)₂F was prepared by reacting CH₂FCH₂OH with trifluoroacetic acid anhydride. Gas chromatography was used to obtain a purified sample.

Malononitrile was purified by recrystallization. Formic acid was dried with Na₂SO₄ prior to use.

Procedure. All of the compounds reported in Table V (except THP) have been subjected to equilibrium constant determinations on the UCI spectrometer system. In addition, many of the equilibrium constants have been independently determined with the Cal Tech spectrometer system. Generally, accord has been excellent, well within the precision measures given. The instrumentation⁸⁻¹² as well as methods and procedures have been previously described,^{5,13-16} at least briefly. A detailed discussion of the procedure utilized with the UCI spectrometer system is given here.

The equilibrium constant for a general thermal proton transfer reaction under the conditions described below is given by

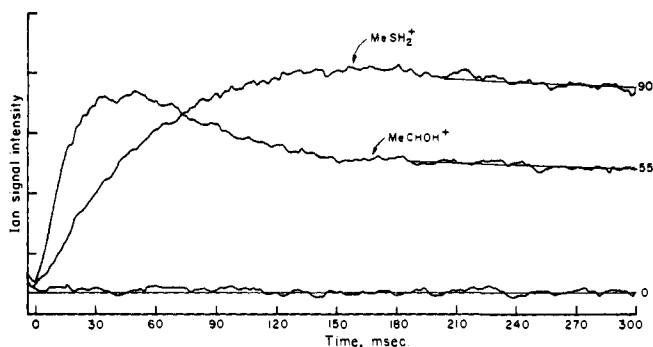
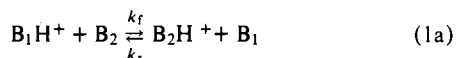


Figure 1. Typical time plot for the determination of the equilibrium constant for the reaction $\text{CH}_3\text{CH}=\text{OH}^+ + \text{MeSH} \rightleftharpoons \text{MeSH}_2^+ + \text{CH}_3\text{CH}=\text{O}$, $p_{\text{MeSH}} = 3.5 \times 10^{-7}$ Torr, $p_{\text{MeCHO}} = 6.9 \times 10^{-7}$ Torr. There is one collision per ion in 20–40 ms. $K_{\text{eq}} = [\text{signal}(\text{MeSH}_2^+)/[\text{signal}(\text{MeCHOH}^+)]](m_{\text{MeSH}_2^+}/m_{\text{MeCHOH}^+})(p_{\text{MeCHO}}/p_{\text{MeSH}}) = (90/55) \cdot (49/45) \cdot (69/35) = 3.5$.



$$K_{\text{eq}} = \left(\frac{\text{B}_2\text{H}^+}{\text{B}_1\text{H}^+} \right)_e \left(\frac{\text{B}_1}{\text{B}_2} \right) = k_f/k_r \quad (1b)$$

where the subscript e denotes the equilibrium state ion abundance ratio and k 's are rate constants.

The standard free energy change for reaction 1a is obtained by

$$-\Delta G^\circ = RT \ln K_{\text{eq}} = RT \ln (k_f/k_r) \quad (2)$$

Pressures of $\sim 10^{-6}$ Torr are maintained for B_1 and B_2 by controlled flow rates through leak valves from a parallel inlet manifold into an ~ 6 -L stainless steel vacuum chamber. The system is pumped at an effective speed of 4 L/s, which results in an average residence time of a neutral molecule in the vacuum system of about 1.5 s. With a wall separation of about 2 cm and an average molecular speed of 3×10^4 cm/s, the wall collisions total about 2×10^4 collisions/particle. This assures thermal equilibrium of the neutral reactant molecules with the inner walls of the spectrometer vacuum system at the mean ambient temperature of 300 K. Both kinetic and equilibrium constant measurements are carried out with the number density of the neutral reactants at least 10^5 -fold greater than that for the ions. Consequently, the partial pressures of B_1 and B_2 are constant throughout an experiment, and the equilibrium ratio, $(\text{B}_1)/(\text{B}_2)$, is determined by utilizing a Bayard-Alpert ionization gauge. This gauge is attached to the analyzer system (cf. subsequent description) by a 10 in. long, 2.5 in. diameter tube in order to minimize any pressure differentials. The gauge was calibrated at pressures higher than 10^{-5} Torr against an MKS Baratron capacitance manometer.

The trapped ion analyzer cell⁸ is contained within the vacuum chamber. This cell serves to generate, trap, and mass analyze gaseous ions in a pulsed mode of operation. The first pulse of ~ 5 ms triggers an electron beam through the interior of the analyzer cell, forming primary ions by electron impact. Following the first pulse is a delay time or reaction period, typically of the order of 300–1000 ms. During the reaction period the analyzer cell acts as a static ion trap. The combined effects of the magnetic field and an electrostatic potential (established inside the cell by DC voltages applied to walls of the cell) trap all ions, primary or secondary ions formed from them by chemical reactions. There is no rf acceleration of the trapped ions by the pulsed marginal oscillator detector during this period. Consequently, no external perturbation of the kinetic energies of the trapped ions occurs during the reaction period. Following the reaction period, a detect pulse is triggered during which ions of a particular m/e are selectively irradiated at their cyclotron frequency by the marginal oscillator. There is a pulsed response from the marginal oscillator which is proportional to the number density of the resonant ions. Following the detect pulse, all ions, regardless of mass, are rapidly neutralized at the walls of the analyzer cell by a quench pulse of 1-ms duration. The quench pulse stops any ion-molecule reactions and prevents ions from one pulse sequence from overlapping into subsequent pulse cycles.

To determine the equilibrium ratio

$$\left(\frac{\text{B}_2\text{H}^+}{\text{B}_1\text{H}^+} \right)_e$$

at a given ratio of a pair of neutral bases, $(\text{B}_1)/(\text{B}_2)$, data are obtained in the form of time plots. The magnetic field strength is adjusted to be in resonance with an ion of given m/e (say B_1H^+), and the abundance of B_1H^+ is monitored as a function of the time of the reaction period by using a scan generator to vary the delay time preceding the detect pulse. Similarly, the abundance of B_2H^+ is followed as a function of reaction time. The transient signals of both B_1H^+ and B_2H^+ are displayed on the Y axis of a recorder. At typical operating pressures on the order of 10^{-6} Torr¹²

$$\text{signal} \propto \frac{Ne^2V\tau}{m}$$

where signal is the drop in the oscillation voltage level in the resonant circuit for N ions of mass-to-charge, m/e , that are irradiated at their cyclotron frequency, τ is the fixed time of duration of the detect pulse, and V is the rf irradiation voltage (also constant for given experiment). Consequently, the ratio of the ion signal intensities at steady state give the equilibrium ion abundances, i.e.

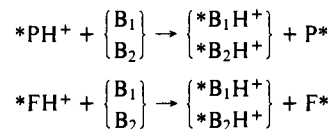
$$\left(\frac{\text{B}_2\text{H}^+}{\text{B}_1\text{H}^+} \right)_e = \frac{[\text{signal}(\text{B}_2\text{H}^+)]_e m_{\text{B}_2\text{H}^+}}{[\text{signal}(\text{B}_1\text{H}^+)]_e m_{\text{B}_1\text{H}^+}}$$

and

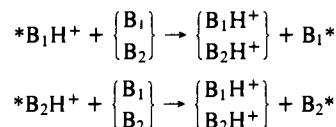
$$K_{\text{eq}} = \frac{[\text{signal}(\text{B}_2\text{H}^+)]_e (m_{\text{B}_2\text{H}^+})(p_{\text{B}_1})}{[\text{signal}(\text{B}_1\text{H}^+)]_e (m_{\text{B}_1\text{H}^+})(p_{\text{B}_2})}$$

In typical experiments, a steady state concentration ratio of the ions prevails within 5 to 50 ion-molecule collisions per ion (200–1000 ms). This steady state ratio condition is further observed up to and beyond 100 collisions per ion in order to confirm that it is a true equilibrium condition. For ions of greatly different mass (e.g., NH_4^+ and $\text{Et-}i\text{-PrOH}_2^+$), the use of nearly constant magnetic field strength has minimized problems of differential ion loss. Figure 1 displays a typical time plot.

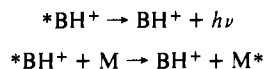
Relaxation to a thermal proton transfer equilibrium (reaction 1a) takes place by both chemical and physical processes. Proton transfer rate constants generally are on the order of 10^{-9} – 10^{-10} $\text{cm}^3 \text{molecule}^{-1} \text{s}^{-1}$.^{17–24} Consequently, the initially formed parent ions, $^*\text{PH}^+$, and fragment ions, $^*\text{FH}^+$, react away very rapidly:



The nonthermalized secondary ions, $^*\text{B}_1\text{H}^+$ and $^*\text{B}_2\text{H}^+$, relax by further proton transfer reactions, i.e.,



That is, proton transfer occurring at nearly every collision provides for a very effective means of momentum transfer and energy relaxation. The relatively long residence times (exceeding those of the ordinary mass spectrometric operation by more than 10^5) provide also for thermal relaxation by several physical processes:¹² damping of ion image currents, radiative emission, and unreactive ion-molecule collisions. The latter two may be represented by



where M is a nonreactive collision partner. Since the proton transfer reactions employed to obtain equilibrium constants (reaction 1) are themselves less exothermic than $3.0 \text{ kcal mol}^{-1}$, there is little or no difficulty from this source in preventing the attainment of thermal proton transfer equilibria. The temperature of the analyzer cell was measured by a thermocouple strapped to the cell.

Evidence that thermal proton transfer equilibria are obtained as a consequence of the above mechanisms of relaxation is provided not only by the time plots but by the observation that the equilibrium constant is independent of the ionizing electron energy, i.e., from 10 to 70 eV—cf. Table I. (We are indebted to Professor E. Grunwald for suggesting this test.)

Rate constants for forward and reverse proton transfer reactions.

Table I. Typical Results Showing Equilibrium Constant to Be Independent of Ionizing Electron Energy

Et- <i>i</i> -PrOH ⁺ + NH ₃ ⇌ NH ₄ ⁺ + <i>i</i> -PrOEt			
Electron energy, eV	ifK _{eq}	Electron energy, eV	K _{eq}
10.8	3.41	50.0	3.16
20.0	3.45	70.0	3.65
30.0	3.65		
av K _{eq} = 3.46 ± 0.15			

Table II. Typical Results Showing Equilibrium Constant to Be Independent of the Concentration Ratio of Base Pairs, i.e., Direction of Approach to Equilibrium

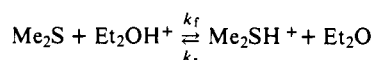
(B ₁)/(B ₂)	K _{eq}
A. Base Pair = THF (B ₁) and EtOAc (B ₂), cf. eq 1	
0.81	8.0
2.14	9.0
3.67	8.5
7.45	8.2
av K _{eq} = 8.4 ± 0.3	
B. Base Pair = <i>i</i> -PrCHO (B ₁) and Me ₂ O (B ₂), cf. eq 1	
0.20	0.82
0.53	0.84
1.02	0.88
2.57	0.88
av K _{eq} = 0.86 ± 0.03	

Table III. Typical Results Showing Equilibrium Constant to Be Independent of Methane Buffer Gas Pressure^a

Et ₂ OH ⁺ + Me ₂ S ⇌ Me ₂ SH ⁺ + Et ₂ O			
10 ⁶ p(CH ₄), Torr	K _{eq}	10 ⁶ p(CH ₄), Torr	k _{eq}
0.0	1.49	60.	1.68
14.1	1.57	111.	1.68
30.	1.54	234.	1.64
av K _{eq} = 1.60 ± 0.07			

^a p(Me₂S) = 3.3 × 10⁻⁷ Torr and p(Et₂O) = 6.2 × 10⁻⁷ Torr

k_f and *k_r*, have been obtained using the pulsed double resonance technique.^{23,25} Illustrating with the Me₂S/EtOH base pair:



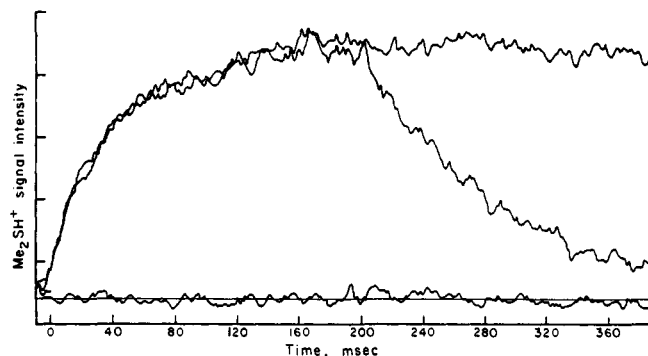
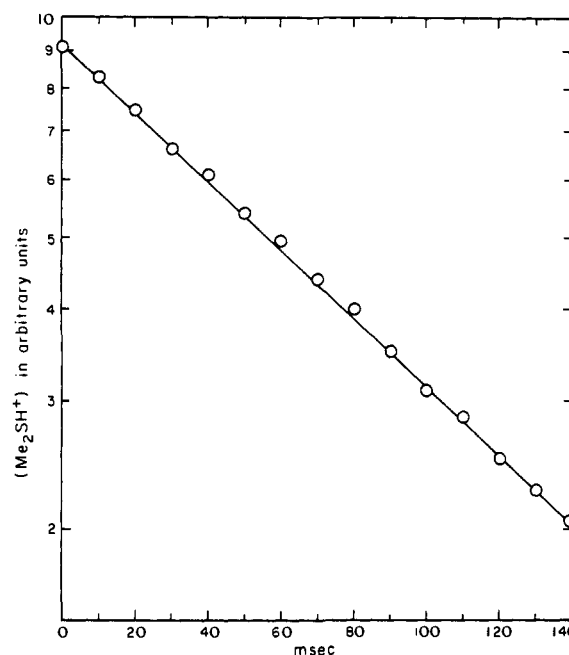
After about 200 ms with Et₂OH⁺ and Me₂SH⁺ at steady state concentrations, a double resonance rf pulse of 0.5 V peak to peak amplitude and of a frequency equal to the cyclotron frequency of the ion to be ejected was applied to the upper plate of the analyzer cell for the balance of the reaction period (another 200 ms). In this manner the desired ion is selectively and completely ejected in a time that is short compared to the time between collisions. The ejection of Me₂SH⁺ results in a logarithmic decay of the Et₂OH⁺ concentration as the reaction shifts to the right.

With (Me₂SH⁺) = 0, for example,

$$\frac{-d(\text{Et}_2\text{OH}^+)}{dt} = k_f(\text{Et}_2\text{OH}^+)(\text{Me}_2\text{S}) = k_{\text{obsd}}(\text{Et}_2\text{OH}^+)$$

where *k_f* is obtained from the pseudo-first-order rate constant, *k_{obsd}*, by dividing by the constant concentration of Me₂S.

The results of a typical ejection experiment are shown in Figure 2. The upper curve shows that the signal for Me₂SH⁺ reaches a steady state abundance in less than 200 ms, and, with no ejection, this is maintained beyond 400 ms. The lower curve shows that the signal obtained for Me₂SH⁺ decays logarithmically as Et₂OH⁺ is ejected at 200 ms. Figure 3 shows a typical semilog plot from which the pseudo-first-order rate constant, *k_{obsd}*, is obtained to evaluate *k_r* (above), i.e., *k_r* = *k_{obsd}*/(Et₂O). (Values so obtained appear in Table IV.)

**Figure 2.** Rate constant determination by ejection of Et₂OH⁺. Reaction: Me₂S + Et₂OH⁺ ⇌ Me₂SH⁺ + Et₂O. p_{Et₂O} = 6.2 × 10⁻⁷ Torr; p_{Me₂S} = 3.3 × 10⁻⁷ Torr. Upper curve—no ion ejection. Lower curve, Et₂OH⁺ completely ejected after 200 ms.**Figure 3.** Typical semilog plot for obtaining pseudo-first-order rate constants from ion ejection experiments.

The low-pressure ICR results reported herein have been successfully and critically tested additionally by six classical means of establishing the equilibrium condition: (1) the equilibrium constants hold to the precision indicated for substantial variations in ratios of the pressures of the neutral bases, typically 1/3 to 3 or greater, cf. Table II (showing, in effect, that the same equilibrium constant is obtained by starting from either side of reaction 1a); (2) the equilibrium constant is independent of total pressure, i.e., there is little or no effect of inert buffer gas (Table III gives typical results); (3) the same equilibrium constant value is obtained from the ratio of the forward and reverse rate constants obtained by selective ion-ejecting experiments (Table IV gives typical results); (4) for a series of bases, the standard free energy change is dependent upon state change only, with no dependence upon route (i.e., B₁ → B₃ is the same as B₁ → B₂ → B₃, etc.—Table V gives a complete summary of these results); (5) for pairs of simple bases for which no entropy change is expected for the gaseous proton transfer reaction, the standard free energy change is independent of temperature, cf. Table VII; (6) generally good accord is obtained by the low-pressure ICR equilibrium constants and those obtained by other methods (cf. ref 4 and 16 and Tables V-VIII).

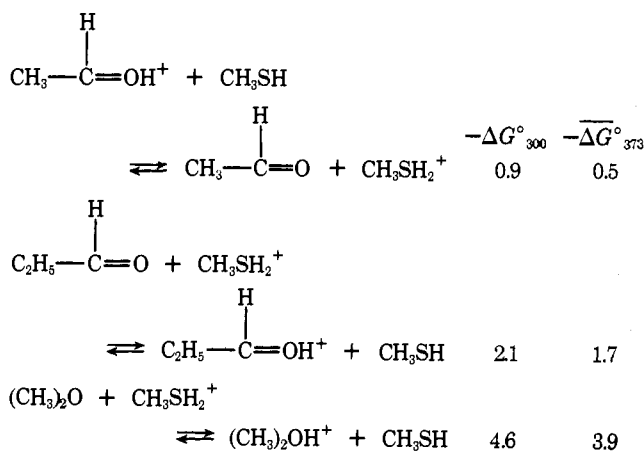
Results

A complete summary of the results of this work is given in Tables V and VI. The equilibrium constant determinations are reported as (2) $-\Delta G^\circ = RT \ln K_{\text{eq}}$. The precision of the in-

dividual K_{eq} values was such that $-\Delta G^\circ$ values are precise to ± 0.2 kcal/mol or less. Table V shows the duplicating overlapping stepwise sequences utilized in this study to determine gas phase basicities between water and ammonia. Agreement between overlapping sequences is found to be well within the combined individual precision measures. Table V gives ΔG° values (rounded to the nearest 0.1 kcal/mol) for the reaction $\text{NH}_4(\text{g})^+ + \text{B}(\text{g}) \rightleftharpoons \text{BH}(\text{g})^+ + \text{NH}_3(\text{g})$ from this work at 300 K and from the work of Kebarle⁴ at 600 K. Also given are ΔH° values obtained from the assumption that the only entropy contributions to ΔS° arise from molecular rotational symmetry numbers (it is assumed that there are no changes in internal rotation symmetry numbers on protonation). The conjugate acids of oxides and sulfides (including H_3O^+) have been taken to have nonplanar trigonal pyramid structures²⁶ in obtaining the molecular rotational symmetry numbers. Table VI gives ΔG° and ΔH° values at 300 K for additional bases which are not included in the overlap sequences.

Particular attention is due the agreement between K_{eq} values obtained from the relative equilibrium ion abundances from the time plots and the k_f/k_r ratio of rate constants (cf. Table IV). These results represent totally different means of evaluating the thermal proton transfer equilibria, and each has different sources of error. For example, values of K_{eq} are dependent upon the accuracy of the calibration of the marginal oscillator at the various resonance frequencies,²⁷ whereas k_f/k_r values are independent of the variable sensitivity of the marginal oscillator. Consequently, the very good accord in $K_{eq} = k_f/k_r$ offers strong confirmation of the methods. The absolute values of the bimolecular rate constants of Table IV are estimated to be reliable to within 20%. The results have been checked against the rate constant for the reaction $\text{CH}_4^+ + \text{CH}_4 \rightarrow \text{CH}_5^+ + \text{CH}_3$ obtained as 1.30 ± 0.02 from $-d\text{CH}_4^+/dt$ and as 1.15 ± 0.06 from $d\text{CH}_5^+/dt$ (over a range of methane pressures of 0.9 to 2.6×10^{-6} Torr) in units of 10^{-9} $\text{cm}^3 \text{ molecule}^{-1} \text{ s}^{-1}$. Literature values^{28,29} for this rate constant are 0.99×10^{-9} , 1.09×10^{-9} , and 1.22×10^{-9} . For reactions in the exothermic direction (as given for each reaction in Table IV), there are trends suggesting somewhat faster rates of proton transfer between simple oxygen bases than between simple nitrogen bases, or between simple sulfur bases. Qualitative observations in obtaining time plots suggest that the rate is slower yet for carbon bases and tends further to be slowed for resonance stabilized bases or bases of high steric requirements.

As discussed further in the following section, there is generally good accord between our ΔH°_{300} and Kebarle's ΔH°_{600} values as given in Tables V and VI. Solka and Harrison³⁰ have recently reported "effective" ΔG°_{373} values for the following three exothermic proton transfer reactions:



However, their method does not involve equilibrium between thermalized ions. There is qualitative agreement with our

ΔG°_{300} values, but as expected for excited ions in an exothermic reaction $-\Delta G^\circ_{373} < -\Delta G^\circ_{300}$ in each case. This result follows from the fact that excess energy promotes the endothermic process at the expense of the exothermic one, tending toward a $\Delta G^\circ = 0$.

Discussion

Comparison of Free Energy of Proton Transfer Obtained by Low-Pressure ICR and by High-Pressure Mass Spectroscopy.

In Table VII the standard free energy of gas phase proton transfer between pairs of typical simple carbon, nitrogen, oxygen, and sulfur bases is compared at 300 and 600 K. The base pairs selected for Table VII involve no entropy effects arising from molecular rotational symmetry numbers. The ΔG° values at 300 K are from this work, and those at 600 K are from the work of Yamdagni and Kebarle.⁴

It is clear from the data of Table VII that ΔG°_{300} and ΔG°_{600} values are very generally equal within the combined experimental uncertainties, a result strongly supporting the validity of both experimental methods. The temperature independence of the ΔG° values of Table VII confirms that proton transfer between simple bases involves very small entropy effects other than those due to molecular rotational symmetry numbers.

Entropy Effects in Gas Phase Proton Transfer Equilibria.

The standard entropy of the proton transfer reaction ($\text{B}_1\text{H}^+ + \text{B}_2 \rightleftharpoons \text{B}_2\text{H}^+ + \text{B}_1$) may be obtained with the assumption that ΔS° has no significant temperature dependence by the relationship

$$\Delta S^\circ = \frac{\Delta G^\circ_{300} - \Delta G^\circ_{600}}{300} \quad (3)$$

Values of ΔS° so obtained are compared in Tables VII and VIII with values of

$$\Delta S^\circ_{\text{rot}} = R \ln \left(\frac{\sigma_{\text{B}_1\text{H}^+} \sigma_{\text{B}_2}}{\sigma_{\text{B}_2\text{H}^+} \sigma_{\text{B}_1}} \right)$$

where σ is the rotational symmetry number. The combined precision measures of ΔG°_{300} and ΔG°_{600} introduce an uncertainty in ΔS° of about ± 1.5 eu. To this precision, there is excellent accord in the approximate equality $\Delta S^\circ \approx \Delta S^\circ_{\text{rot}}$, for all base pairs of Table VIII.

We have noted several base pairs for which accord between ΔS° and $\Delta S^\circ_{\text{rot}}$ is well outside of ± 1.5 eu and are reinvestigating (in collaboration with Professor Kebarle) the results for these bases. Included are the following pairs: $\text{HCO}_2\text{H}-\text{MeOH}$ and $\text{H}_2\text{O}-\text{CF}_3\text{CO}_2\text{H}$. Clearly, however, the present results provide strong evidence that entropy effects in gas phase proton transfer between simple bases (bifunctional bases forming chelates are excluded)^{16,31-33} are generally quite small and readily predictable in terms of changes in molecular rotational symmetry numbers.

Relative Proton Affinities of Hydrides. The stair-stepping overlap manifold of gas phase proton transfer equilibria of Table V gives a gas phase basicity of water (ΔG°_{300} of Table V) which is 31.4 kcal mol⁻¹ less than that for ammonia. With correction for rotational symmetry numbers, the proton affinity of water (ΔH°_{300} of Table V) is 32.0 kcal mol⁻¹ less than that of ammonia. Considering possible cumulative errors in the overlaps (random errors should be largely eliminated by the multiple overlaps), we believe this figure to be accurate to ± 1.0 kcal mol⁻¹. While this work was in progress, Yamdagni and Kebarle⁴ have reported $\Delta\text{PA} = 31.5 \pm 1-2$ kcal,³⁴ from their high-pressure mass spectrometric studies at 600 K. The agreement is clearly excellent and supports the validity of both methods. In a separate publication,⁶ the relative proton affinities are combined with critically evaluated absolute proton affinities for a number of bases. This procedure has given PA

Table IV. Rate and Equilibrium Constants from Pulsed Ion Ejection Experiments

Proton transfer reaction	$10^9 k_f^a$	$10^{10} k_r^a$	k_f/k_r^b	K_{eq}^c
$H_3O^+ + CF_3CH_2OH \xrightleftharpoons{k_f} CF_3CH_2OH_2^+ + H_2O$	3.47	0.98	35.5	34.4 ± 1.9
$CF_3CH_2OH_2^+ + H_2S \xrightleftharpoons{k_r} H_3S^+ + CF_3CH_2OH$	1.10	0.89	12.4	12.7 ± 0.5
$Et_2OH^+ + EtOAc \rightleftharpoons EtOAcH^+ + Et_2O$	3.02	15.6	1.94	1.96 ± 0.13
$Me_2SH^+ + EtOAc \rightleftharpoons EtOAcH^+ + Me_2S$	0.70	5.90	1.19	1.22 ± 0.15
$Et_2OH^+ + Me_2S \rightleftharpoons Me_2SH^+ + Et_2O$	0.82	5.89	1.40	1.36 ± 0.17
$Et-i-PrOH^+ + NH_3 \rightleftharpoons NH_4^+ + Et-i-PrO$	1.03	3.09	3.33	3.46 ± 0.15

^a In cm^3 molecule⁻¹ s⁻¹. ^b Estimated uncertainty 10%. ^c K_{eq} from time plot steady state ion abundances.

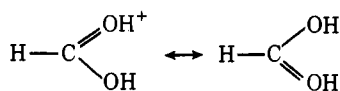
(H_2O) = 170.3 ± 2 kcal mol⁻¹ and PA (NH_3) = 202.3 ± 2 kcal mol⁻¹.

Of interest are the periodic trends in the proton affinities, i.e., the ionic heterolytic bond dissociation energies ($BH^+ \rightarrow B: + H^+$, given as $D_{(BH^+)} = PA$, for emphasis), and in the corresponding homolytic bond dissociation energies ($BH^+ \rightarrow B^{\cdot+} + H\cdot$; $D_{(B^{\cdot+})}$), which are derived from the PAs and the first adiabatic ionization potentials (IP).³⁵

$$D_{(B^{\cdot+})} = D_{(BH^+)} + IP_{(B)} - IP_{(H)} \quad (4)$$

A summary of $IP_{(B)}$, $D_{(B^{\cdot+})}$, and $D_{(BH^+)}$ values is given in Table IX. Literature values are given for the compounds not studied in this work. Overall there are strong trends for $D_{(BH^+)}$ to decrease and $D_{(B^{\cdot+})}$ to increase as $IP_{(B)}$ increases. However, some clear exceptions may be noted. In group 5, as $IP_{(B)}$ decreases with increasing period number, values of $D_{(BH^+)}$ decrease by even larger amounts. Further, for group 5 elements of the third and fourth periods (P and As), values of $D_{(B^{\cdot+})}$ are greater than for the corresponding group 6 elements (S and Se) even though the corresponding $IP_{(B)}$ values are in the reverse (normal) orders. The pattern of $D_{(BH^+)}$ values has been rationalized by McDaniel³⁶ as resulting from two opposed effects: increasing electronegativity which decreases $D_{(BH^+)}$ (clearly predominant for group 8 and 7 ions, and slightly predominant for group 6 ions) and an electron-releasing effect of the bonded hydrogen atoms which increases $D_{(BH^+)}$ the greater the number of hydrogen atoms and the greater the electronegativity of the element (predominant for the group 5 ions).

Organic Functional Group Proton Affinities. The results of this work make possible for the first time a comparison of precise relative proton affinities for a number of organic functional groups bearing the simplest of all substituents—the hydrogen atom. The results arranged in order of increasing base strength are as follows: H_2O (−32.0), H_2S (−28.4), $HC\equiv N$ (−27.8), $H_2C=O$ (−27.7), HCO_2H (−22.2), C_6H_6 (−20.9), H_3P (−14.9), H_3N (0.0). The proton affinity tends to decrease as the electronegativity of the element with the lone pair of electrons increases. The equivalent PAs of HCN and H_2CO suggest essentially equivalent electronegativities of sp nitrogen and sp² oxygen. This conclusion appears to be in excellent accord with the valence state electronegativities assigned by Moffitt.³⁷ Other influences are also evident. For example, conjugative interactions in BH^+ are important in that the PA of HCO_2H is 5.5 kcal greater than that of H_2CO . Since the OH substituent in HCO_2H should decrease PA by inductive-electronegativity considerations, the greater PA must be due to a predominant stabilization effect of conjugative charge delocalization.



Experimental results⁴⁵ in mineral acid solutions and ab initio molecular orbital calculations⁴⁶ indicate that protonation

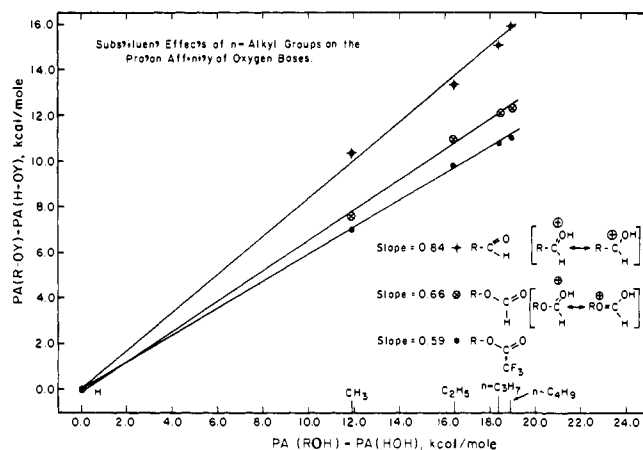


Figure 4. Substituent effects of *n*-alkyl groups on the proton affinity of oxygen bases: \blacklozenge , Y = aldehyde, CHO; \otimes , Y = formate, OOC; \bullet , Y = trifluoroacetate, OOCF₃.

occurs at the carbonyl oxygen (cf. below for gas phase evidence).

The presence of only H atom substituents minimizes polarizability and polarity effects upon proton affinities.^{16,47,55} Consequently, effects of hybridization on proton affinity can be estimated more quantitatively from present results. The proton affinity of CH_3OH is 7.6 kcal mol⁻¹ greater than that for $H_2C=O$. The figure 7.6 kcal provides a quantitative estimate (upper limit) for the effect on PA of the change between $\sim sp^2$ and $\sim sp^3$ hybridization of oxygen and its bonded carbon atom. Aue obtained the figure 5.7 kcal for such a hybridization change of nitrogen and bonded carbon atoms based upon PA (piperidine) – PA (pyridine).⁴⁸ The proton affinity of CH_3NH_2 is ~ 9 kcal mol⁻¹ greater than that of $CH_2=NH$,⁴⁹ and 36.7 kcal mol⁻¹ greater than that of $HC\equiv N$. The figures 9 and 36.7 kcal mol⁻¹ provide quantitative estimates (upper limits) for the effect on PA of the hybridization change from $\sim sp^3$ to $\sim sp^2$ and from $\sim sp^3$ to $\sim sp$, respectively, for nitrogen and its bonded carbon atom.

Substituent Effects of Normal Alkyl Groups and Site of Ester Protonation. The present results make available precise figures for the effects of *n*-alkyl substituents relative to H on proton affinities for four different series of oxygen functional groups. In each series, PA increases in the sequence $H < Me < Et < n-Pr < n-Bu$, with successively diminishing effects. The same sequence has been observed for amines^{16,47} and nitriles.⁵⁰ These alkyl substituent effects are given in Table X for each of the four series HOH, HO_2CCF_3 , HO_2CH , and HCHO. In Figure 4, these results are shown plotted for the latter three series vs. the former. Approximately linear relationships are observed with the variable slopes indicated. For water and the alcohols, protonation must occur on the atom (oxygen) to which the substituent is directly attached. For the aldehyde series, the carbonyl carbon atom intervenes between the pro-

Table V. Standard Free Energies and Enthalpies of Proton Transfer and Proton Affinities Relative to Ammonia (kcal mol⁻¹)
 $\text{NH}_4^+ + \text{B} \rightleftharpoons \text{BH}^+ + \text{NH}_3$

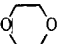
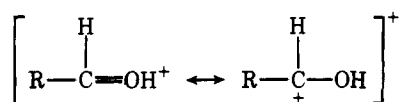
Base	Directly measured ΔG°_{300}	ΔG°_{300}	ΔH°_{300}	ΔG°_{600}	ΔH°_{600}
NH ₃		0.0	0.0	0.0	0.0
<i>i</i> -PrOEt	0.8	0.8	1.6		
CF ₃ CH ₂ NH ₂	1.0	1.8	2.0		
EtOAc	1.6	3.4	4.2	2.7	4.3
Me ₂ S	0.1	3.5	4.7		
Et ₂ O	0.2	3.7	4.9	2.6	5.0
THP	0.9	4.0	5.2		
THF	0.7	4.7	5.9		
MeOAc	1.4	6.1	6.9	5.3	6.9
Me ₂ CO	1.1	7.2	8.4	6.1	8.5
MeOEt		7.5	8.3		
Me ₂ C=CH ₂	1.5	8.6	8.8	7.7	8.1
HCO ₂ - <i>n</i> -Bu	0.4	9.0	9.8		
HCO ₂ - <i>n</i> -Pr	0.2	9.2	10.0	9.0	10.6
		9.8	11.4		
HCO ₂ Et	0.5	10.3	11.1	9.5	11.1
<i>i</i> -PrCHO	0.5	10.9	11.7		
<i>n</i> -BuCHO	0.0	10.9	11.7		
Me ₂ O		11.0	12.2	10.6	13.0
<i>n</i> -PrCHO	0.7	11.8	12.6		
EtCHO	1.7	13.5	14.3	12.8	14.4
HCO ₂ Me	0.3	13.8	14.6	12.9	14.5
MeCN	0.7	14.5	15.3	13.3	14.9
EtOH		14.8	15.6	13.9	15.5
PH ₃	0.1	14.9	14.9		

Table V (Continued)

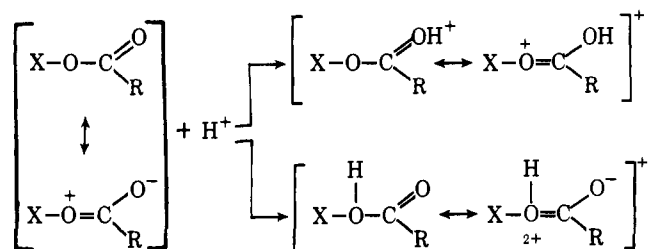
Base	Directly measured ΔG°_{300}	ΔG°_{300}	ΔH°_{300}	ΔG°_{600}	ΔH°_{600}
MeCHO		16.5	17.3	15.3	16.9
CF ₃ CO ₂ - <i>n</i> -Bu		17.1	17.9		
CF ₃ CO ₂ - <i>n</i> -Pr		17.3	18.1		
CF ₃ CO ₂ Et		18.3	19.1		
MeOH		19.3	20.1	18.6	20.2
NCCO ₂ Et		20.6	21.4		
ClCH ₂ CN		20.6	21.4		
HCO ₂ CH ₂ CF ₃		20.7	21.5		
CF ₃ CO ₂ Me		21.2	22.0		
AsH ₃		21.4	21.4		
HCO ₂ H		21.8	22.2	22.6	23.4
CCl ₃ CH ₂ OH		22.5	23.3		
F ₂ CHCH ₂ OH		23.6	24.4		
CCl ₃ CN		24.0	24.8		
CH ₂ (CN) ₂		24.2	24.6		
H ₂ CO		26.5	27.7		
HCN		27.0	27.8		
H ₂ Se		27.0	27.6		
H ₂ S		27.8	28.4	28.7	29.9
CF ₃ CH ₂ OH		29.3	30.1		
H ₂ O		31.4	32.0	31.8	33.0

tonated oxygen atom and the substituent. As expected, therefore, the slope of the aldehyde family in Figure 4 is less than unity. The slope of 0.84, however, represents a small "fall-off" factor for the carbonyl carbon. This result is readily understood, however, in terms that an appreciable delocalization of positive charge to the carbonyl carbon will occur as represented by the resonance forms:



For the two ester families, either the carbonyl oxygen or the alcoholic oxygen is a potential site of protonation.

The resonance forms suggest that protonation occurs at the carbonyl oxygen since in this form resonance stabilization in



the ester function is preserved and enhanced. For protonation on the alcoholic oxygen, resonance stability is pictured as

Table VI. Standard Free Energies and Enthalpies of Proton Transfer and Proton Affinities Relative to Ammonia for Additional Bases (kcal mol⁻¹)

Base	Reference base	ΔG°_{300}	ΔH°_{300}	ΔG°_{600}	ΔH°_{600}
CF ₃ CO ₂ H	H ₂ S ^a	28.6	29.0		
ClCN	F ₂ CHCH ₂ OH ^b	24.1 ± 0.5	24.9 ± 0.5		
CF ₃ CO ₂ (CH ₂) ₂ F	F ₂ CHCH ₂ OH ^a	21.4	22.2		
C ₆ H ₆	MeOH ^a	19.0	20.9	17.3	21.1
MeSH	MeCHO ^a	15.6	16.4		
Cl(CH ₂) ₂ CN	MeCN ^b	15.4	16.2		
HOAc	MeCN ^a	13.9	14.3	13.3	14.1
CH ₂ =CHCN	MeCN ^b	13.6	14.4		
C ₆ H ₅ Me	HCO ₂ Me ^c	12.8	13.6		
C ₆ H ₅ Et	C ₆ H ₅ Me ^c	11.9	12.7		
EtCN	HCO ₂ Et, Me ₂ O ^b	11.3	12.1		
C ₆ H ₅ - <i>n</i> -Pr	C ₆ H ₅ Et ^c	11.1	11.9		
C ₆ H ₅ - <i>n</i> -Bu	C ₆ H ₅ - <i>n</i> -Pr ^c	10.7	11.5		
<i>n</i> -PrCN	HCO ₂ Et, Me ₂ O ^b	10.1	10.9		
<i>o</i> -Xylene	C ₆ H ₅ - <i>n</i> -Bu ^c	10.0	11.2		
<i>n</i> -BuCN	HCO ₂ Et ^b	9.6	10.4		
<i>i</i> -PrCN	HCO ₂ Et ^b	9.3	10.1		
<i>c</i> -C ₃ H ₅ CN	HCO ₂ - <i>n</i> -Bu ^b	8.3	9.1		
<i>c</i> -C ₃ H ₅ CH=CH ₂	Me ₂ CO ^d	6.3	7.1		
(MeO) ₂ CO	EtOAc, Et ₂ O ^e	3.9	5.1		
C ₆ H ₅ CH=CH ₂	CF ₃ CH ₂ NH ₂ ^d	2.2	3.0		
MePH ₂	CF ₃ CH ₂ NH ₂ ^f	0.3	0.5		

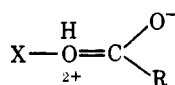
^a This work. ^b Reference 50. ^c Reference 43. ^d Reference 15. ^e Reference 51. ^f Reference 59.

Table VII. Temperature Independence Values of ΔG° for Proton Transfer Equilibria

$B_1H^+ + B_2 \rightleftharpoons B_2H^+ + B_1$					
B ₁	B ₂	$-\Delta G^\circ_{300}$, kcal ^a	$-\Delta G^\circ_{600}$, kcal ^b	ΔS° , eu ^c	ΔS°_{rot} , eu ^d
MeOAc	EtOAc	2.7	2.6	-0.3	0.0
HCO ₂ Et	EtOAc	6.9	6.8	-0.3	0.0
HCO ₂ Me	EtOAc	10.4	10.2	-0.7	0.0
Et ₂ O	Me ₂ CO	-3.5	-3.5	0.0	0.0
HCO ₂ Me	EtCHO	0.3	0.1	-0.7	0.0
MeOH	EtCHO	5.8	5.8	0.0	0.0
HCO ₂ Et	EtOH	-4.5	-4.4	+0.3	0.0
MeCN	EtOH	-0.3	-0.6	-1.0	0.0
MeCHO	EtOH	1.7	1.4	-1.0	0.0
EtOH	MeOH	-4.5	-4.7	-0.7	0.0
MeOAc	MeOH	-13.2	-13.3	-0.3	0.0
HCO ₂ Me	MeOH	-5.5	-5.7	-0.7	0.0
H ₂ O	H ₂ S	3.6	3.1	-1.7	0.0

^a Present results. ^b Yamdagni and Kebarle, ref 4. ^c $\Delta S^\circ = (\Delta G^\circ_{300} - \Delta G^\circ_{600})/300$. ^d $\Delta S^\circ_{rot} = R \ln [(\sigma_{B_1H} + \sigma_{B_2})/(\sigma_{B_2H} + \sigma_{B_1})]$.

having been diminished (form



presumably being of little importance). This conclusion is supported by experimental observations^{45,52} in anhydrous acid media, which show that the carbonyl oxygen is preferentially protonated. On the other hand, Pesheck and Buttrill⁵³ have inferred alcoholic oxygen protonation of esters in the gas phase. Their kinetic evidence is not conclusive regarding the favored site of protonation since the decay mode observed is for a chemically activated species whose internal energy greatly exceeds the difference in PAs of the two ether oxygens. Thomas et al.⁵⁴ conclude on the basis of a correlation between oxygen IS ionization potentials and proton affinities that protonation occurs favorably at the carbonyl oxygen.

Our proton affinity results also favor the latter conclusion. Protonation of the alcoholic oxygen (the atomic center bearing the substituent group) would be expected to lead to a slope in

Figure 4 of near unity (e.g., nearly the same substituent effects as for the water-alcohol family). Instead, slopes of only 0.66 (formate esters) and 0.59 (trifluoroacetate esters) are observed. These slopes, although very appreciably less than unity, are still large compared to the factor expected $\sim(1/2)^2$ in a saturated system for the 1,3 relationship between protonation and substituent sites.¹⁶ However, the observed slopes are readily understood in terms of the expected delocalization of positive charge to the alcoholic oxygen in the carbonyl oxygen protonated form (cf. resonance forms above). While polarization effects undoubtedly predominate generally in the *n*-alkyl substituent effects discussed in this section,^{16,55} there are probably significant contributions from hyperconjugative (especially for the RCHO series) and internal inductive effects (alkyl groups exerting electron-releasing effects through the σ bond). Separation of these effects will be the subject of subsequent publications. For purposes of the present qualitative arguments, the total observed effects of the *n*-alkyl groups suffice, however.

Hydride Affinities of Carbocations. The present results

Table VIII. Entropy Effects in Proton Transfer Equilibria Given by Rotational Symmetry Number Effects

$B_1H^+ + B_2 \rightleftharpoons B_2H^+ + B_1$					
B_1	B_2	$-\Delta G^\circ_{300}, \text{kcal}^a$	$-\Delta G^\circ_{600}, \text{kcal}^b$	$\Delta S^\circ, \text{eu}^c$	$\Delta S^\circ_{\text{rot}}, \text{eu}^d$
Et ₂ O	NH ₃	3.7	2.6	-3.7	-4.1
Me ₂ CO	NH ₃	7.2	6.1	-3.7	-4.0
EtCHO	NH ₃	13.5	12.8	-2.3	-2.7
EtOH	NH ₃	14.8	13.9	-3.0	-2.7
MeOH	NH ₃	19.3	18.6	-2.3	-2.7
C ₆ H ₆	NH ₃	19.0	17.3	-5.7	-6.3
MeOH	Me ₂ CO	12.1	12.5	+1.3	+1.4
C ₆ H ₆	MeOH	-0.3	-1.3	-3.3	-3.6
H ₂ S	HCO ₂ H	6.0	6.1	+0.3	-0.5
H ₂ O	HCO ₂ H	9.6	9.2	-1.3	-0.5
H ₂ O	Me ₂ O	20.4	21.2	+2.7	+2.2

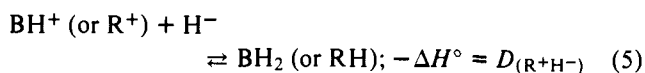
^a Present results. ^b Yamdagni and Kebarle, ref 4. ^c $\Delta S^\circ = (\Delta G^\circ_{300} - \Delta G^\circ_{600})/300$. ^d $\Delta S^\circ_{\text{rot}} = R \ln [(\sigma_{B_1H} + \sigma_{B_2})/(\sigma_{B_2H} + \sigma_{B_1})]$.

Table IX. Heterolytic and Homolytic Bond Dissociation Energies for Conjugate Acid Ions (BH⁺), in kcal mol⁻¹ at 298 K

	NH ₄ ⁺	H ₃ O ⁺	H ₂ F ⁺	HeH ⁺
IP(B) ^g				567.0
D(BH ⁺)				43.3 ^a , ^b
D(B ⁺ A)				296.8
				NeH ⁺
IP(B) ^g	234.3	290.6	369.2	497.2
D(BH ⁺)	202.3 ^h	170.3	112.7 ^d	48.9 ^a , ^b
D(B ⁺ A)	122.9	147.2	168.3	232.6
				ArH ⁺
IP(B) ^g	229.7	240.5	293.8	363.4
D(BH ⁺)	187.4	173.9	136. ^e	89.8 ^b
D(B ⁺ H)	103.4	100.8	116.2	139.6
				KrH ⁺
IP(B) ^g	228.	227.8	269.6	322.8
D(BH ⁺)	180.9	174.7	140. ^e	99.8 ^b
D(B ⁺ H)	95.3	88.9	95.9	109.0
				XeH ⁺
IP(B) ^g			239.4	279.7
D(BH ⁺)			147. ^f	113.2 ^c
D(B ⁺ A)			73.	79.2

^a Reference 38. ^b Reference 39. ^c Reference 40. ^d Reference 41. ^e Reference 42. ^f Reference 3. ^g Reference 44. ^h Reference 6. The estimated uncertainty of ± 2 kcal leads to similar (or greater) uncertainties for all other values of $D(\text{BH}^+)$.

provide a means for further accurate evaluation of gaseous ion thermochemical data. In selected cases, e.g., B = olefins and carbonyl compounds, the hydride affinities ($D_{(\text{BH}^+\text{H}^-)}$) for substituted methyl cations may be obtained. The hydride affinity is defined by the following reaction:



Therefore, the following thermochemical equations are applicable:

$$\begin{aligned} \Delta H^\circ_{(5)} &= \Delta H_{f(\text{BH}_2)} - \Delta H_{f(\text{R}^+)} - \Delta H_{f(\text{H}^-)} = -D_{(\text{R}^+\text{H}^-)} \\ \Delta H_{f(\text{R}^+)} &= \Delta H_{f(\text{B})} - D_{(\text{BH}^+)} + \Delta H_{f(\text{H}^+)} \end{aligned} \quad (6)$$

Therefore

$$\begin{aligned} D_{(\text{R}^+\text{H}^-)} &= \Delta H_{f(\text{B})} - \Delta H_{f(\text{BH}_2)} \\ &\quad - D_{(\text{BH}^+)} + \Delta H_{f(\text{H}^-)} + \Delta H_{f(\text{H}^+)} \end{aligned} \quad (7a)$$

or

$$D_{(\text{R}^+\text{H}^-)} = \Delta H^\circ_{(\text{H}_2)} - D_{(\text{BH}^+)} + 400.4 \quad (7b)$$

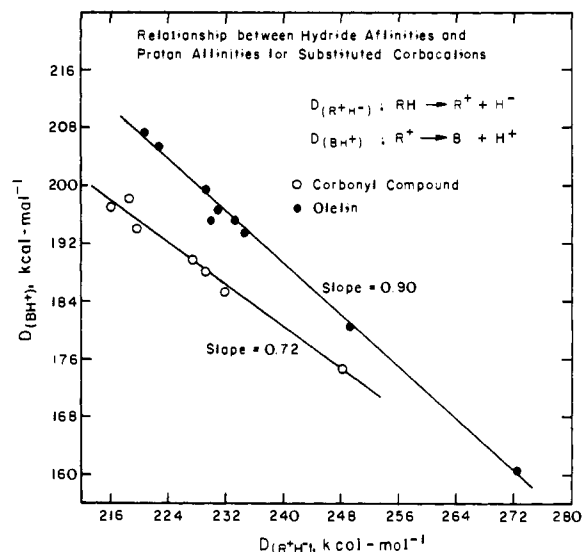


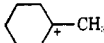
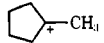
Figure 5. Relationship between hydride affinities and proton affinities for substituted carbocations: closed circles, olefins; open circles, carbonyl compounds.

where $\Delta H^\circ_{(\text{H}_2)}$ is the standard heat of hydrogenation of B (to give $\text{BH}_2 = \text{RH}$). These heats of hydrogenation are available either from direct measurements⁵⁶ or from the difference in the heats of formation of B and BH_2 (eq 7a). It is readily seen that the effects of molecular structure on $D_{(\text{R}^+\text{H}^-)}$ differ from corresponding effects on the proton affinity, $D_{(\text{BH}^+)}$, by the effects on the heats of hydrogenation. It has been well established that structural effects on the latter are generally relatively small compared to corresponding structural effect on the proton affinity. Consequently, some degree of correlation is expected between $D_{(\text{R}^+\text{H}^-)}$ values and corresponding $D_{(\text{BH}^+)}$ values. Table XI summarizes these values for both olefins and carbonyl compounds. Figure 5 shows $D_{(\text{R}^+\text{H}^-)}$ values plotted vs. $D_{(\text{BH}^+)}$. Relatively precise linear relationships are found. Separate lines appear in Figure 5 for olefins and carbonyl compounds, since $D_{(\text{BH}^+)}$ involves a heterolytic bond dissociation energy for a CH with the former and an OH bond with the latter. Scatter from the linear correlations must arise from nonlinear relationships between $\Delta H_{(\text{H}_2)}$ and corresponding $D_{(\text{BH}^+)}$ values. Structural effects for these two quantities are expected to involve different combinations of polarizability, polarity, hyperconjugation, conjugation, and ring strain energies. Even so, these two quantities tend to run very crudely parallel as Table XI shows. The slope (0.90) for olefins in Figure 5 is appreciably larger than that (0.72) for the carbonyl

Table X. Effects of *n*-Alkyl Substituents on the Proton Affinities of Water, Formic and Trifluoroacetic Acid, and Formaldehyde

HOH	0.0	HO ₂ CCF ₃	(0.0)	HO ₂ CH	(0.0)	HCHO	(0.0)
MeOH	11.9	MeO ₂ CCF ₃	7.0	MeO ₂ CH	7.6	MeCHO	10.4
EtOH	16.4	EtO ₂ CCF ₃	9.9	EtO ₂ CH	11.1	EtCHO	13.4
<i>n</i> -PrOH	18.5 ⁵¹	<i>n</i> -PrO ₂ CCF ₃	10.9	<i>n</i> -PrO ₂ CH	12.2	<i>n</i> -PrCHO	15.1
<i>n</i> -BuOH	19.0 ⁵¹	<i>n</i> -BuO ₂ CCF ₃	11.1	<i>n</i> -BuO ₂ CH	12.4	<i>n</i> -BuCHO	16.0
<i>m</i>	(1.00)	0.66		0.59		0.84	

Table XI. Heats of Formation, Proton Affinities, and Hydride Affinities for Substituted Methyl Cations (in kcal mol⁻¹, 298 K)

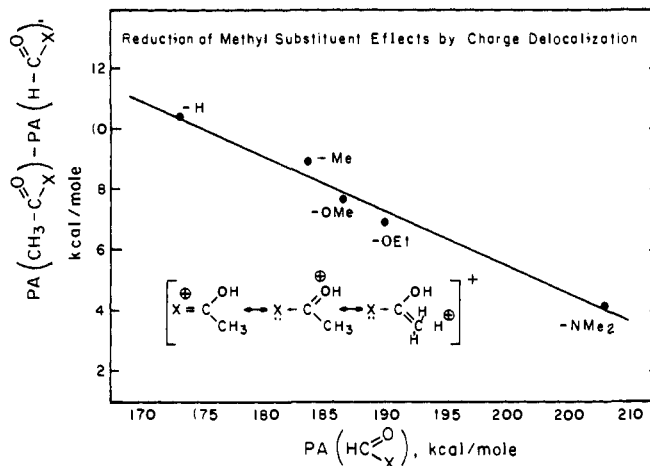
R ⁺	ΔH _f (R ⁺)	ΔH(H ₂) ^a	D(BH ⁺) ^b	D(BH ⁺ H ⁺) ^c
Olefins				
CH ₃ CH ₂ ⁺	218.9 ^d	32.6	160.6	272.5
(CH ₃) ₂ CH ⁺	191.5 ^d	29.9	180.4	249.7
(CH ₃) ₃ C ⁺	169.2	27.9	193.5	234.8
CH ₂ (Δ)CH ⁺		28.1	195.2 ^e	233.3 ^d
	160.4	27.0	196.6 ^f	230.8
	169.4	24.5	195.9 ^f	229.9
CH ₃ (C ₆ H ₅)CH ⁺	202.9	28.1	199.3 ^e	229.2
(CH ₃) ₂ (C ₆ H ₅)C ⁺	188.8	26.0	205.2 ^e	221.3
(CH ₃) ₃ (Δ)C ⁺		27.5	207.1 ^e	220.8 ^e
Aldehydes and Ketones				
HOCH ₂ ⁺	166.4	22.0	174.6	247.8
HO(CH ₃)CH ⁺	142.3	16.5	185.0	231.9
HO(Et)CH ⁺	134.5	16.8	188.0	229.2
HO(<i>n</i> -Pr)CH ⁺	128.4	16.8	189.7	227.5
HO(Me) ₂ C ⁺	121.2	13.0	193.9	219.5
HO(C ₆ H ₅)CH ⁺	162.8	16.5	198.2 ^g	218.7
HO(CH ₃)(C ₂ H ₅)C ⁺	113.0	12.8	197.0 ^g	216.2

^a Values taken from ref 56, or from ΔH_f(B) - ΔH_f(BH₂) as given by S. W. Benson et al., *Chem Rev.*, 69, 279 (1969). ^b Based upon PA(NH₃) = 202.3 ± 2; cf. ref 6. ^c Based upon eq 7b with ΔH_f(H⁺) = 367.2 and ΔH_f(H⁻) = 33.2 kcal mol⁻¹; cf. "JANAF Thermochemical Tables", 2nd ed, NSRD-NBS 37, 1971. ^d F. P. Lossing and G. P. Semeluk, *Can. J. Chem.*, 48, 955 (1970). ^e J. F. Wolf, P. G. Harch, R. W. Taft, and W. J. Hehre, *J. Am. Chem. Soc.*, 97, 2902 (1975). ^f S. K. Pollack, J. F. Wolf, B. A. Levi, R. W. Taft, and W. J. Hehre, *ibid.*, 99, 1350 (1977). ^g Reference 51.

Table XII. Methyl Substituent Effects on Proton Affinity, δ_{Me}D(BH⁺) = PA(CH₃Y) - PA(HY)

Base, RY R = CH ₃ , H	δ _{Me} D(BH ⁺), kcal/mol	D(HYH ⁺), kcal/mol
RCH=CH ₂	19.8	160.6
RPH ₂	14.4	187.4
RCN	12.5	174.5
ROH	11.9	170.3
RSH	12.0	173.9
RCHO	10.4	174.6
RNH ₂	9.0 ¹⁶	(202.3) ⁶
RCOCH ₃	8.9	185.0
RCO ₂ Me	7.7	187.7
RO ₂ CH	7.6	180.1
RO ₂ CMe	7.4	188.7
RO ₂ CCF ₃	7.0	173.3
RCO ₂ C ₂ H ₅	6.9	191.2
RCONMe ₂	4.0 ¹⁶	209.8 ¹⁶

compounds. Since the C=O bond is more polar than the C=C bond, there are larger structural effects, e.g., hyperconjugation, conjugation, and polarity, on the heats of hydrogenation⁵⁷ and thus smaller structural effects on the proton affinities of the

**Figure 6.** Reduction of methyl substituent effects by charge delocalization in protonated carbonyl compounds. Substituent X is as given.

carbonyl compounds (cf. subsequent discussion of methyl substituent effects).

Methyl Substituent Effects. The precise relative proton affinities obtained in this work provide new quantitative comparisons of alkyl substituent effects, the methyl substituent effect on PA having been extensively evaluated for various organic functional groups. The results together with some additional literature data are given in Table XII.

Methyl substituent effects on PA in Table XII vary by about fivefold, being largest for carbonium ion formation from olefins and least for protonation of *N,N*-dimethyl amides. The magnitude of the methyl substituent effect on PA is in general unrelated to proton affinity of the parent hydrogen substituted functional group as shown in Table XII. However, within families of bases methyl effects may decrease regularly with increasingly basic functional groups. This is illustrated in Figure 6 for the carbonyl series RCHO, RMeCO, RCO₂Me, RCO₂Et, and RCONMe₂. The linear relationship of Figure 6 further supports our contention that gas phase protonation of the ester (and the amide⁵⁸) occurs preferentially at the carbonyl oxygen. The former two members of the series must protonate at this position, but the latter two members could protonate at the alcoholic oxygen or the amide nitrogen. However, if the latter sites of protonation were preferentially favored, nearly the same acyl methyl substituent effects should prevail for these two members. Instead, the methyl substituent effect observed for the amides is appreciably less than that observed for the esters. This result, as well as the linear relationship observed for the entire family, is expected for preferential carbonyl oxygen protonation, since increasing ability of the substituent, X, to stabilize the positive charge of conjugate acids of such structures will systematically reduce the stabilizing effects of the methyl (R) substituent:

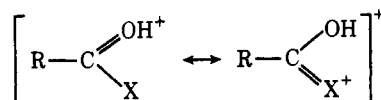


Table XIII. Substituent Effects on Heterolytic and Homolytic Bond Dissociation Energies for the Conjugate Acids of *n*-Bases (kcal mol⁻¹)

RY	IP _(B)	<i>D</i> _(BH⁺)	<i>D</i> _(B⁺H)	δ _{Me} <i>D</i> _(BH⁺)	-δ _{Me} <i>D</i> _(B⁺H)
H ₂ O	290.6 ⁴⁴	170.3	147.2		
CH ₃ OH	250.7 ⁴⁴	182.2	119.3	11.9	27.9
(CH ₃) ₂ O	229.7 ⁴⁴	191.1	106.2	7.9	13.1
NH ₃	234.3 ⁶⁰	202.3	122.9		
CH ₃ NH ₂	206.8 ⁶⁰	211.3	104.5	9.0	18.4
(CH ₃) ₂ NH	190.0 ⁶⁰	217.9	94.3	6.6	10.2
(CH ₃) ₃ N	181.5 ⁶⁰	222.1	90.0	4.2	4.3
H ₂ S	240.5 ⁴⁴	173.9	100.8		
CH ₃ SH	217.7 ⁴⁴	185.8	90.0	12.0	10.8
(CH ₃) ₂ S	200.4 ⁴⁴	197.6	84.4	11.7	5.6
PH ₃	229.6 ⁵⁹	187.4	103.4		
CH ₃ PH ₂	210.2 ⁵⁹	201.8	98.4	14.4	5.0
(CH ₃) ₂ PH	195.3 ⁵⁹	214.0	95.7	12.2	2.7
(CH ₃) ₃ P	184.7 ⁵⁹	223.5	94.6	9.5	1.1
AsH ₃	228. ⁴⁴	180.9	95.		
(CH ₃) ₃ As	182. ⁶¹	210.7 ⁶¹	79.	29.8	16.

Methyl substituent effects on homolytic bond dissociation energies and certain hydride affinities for BH⁺ ions are highly instructive and have been evaluated using eq 4 and 7. The expressions for the methyl substituents effects simplify to eq 8 and 9, which illustrate the improved precision (and, presumably, accuracy) which follows from use of relative values.

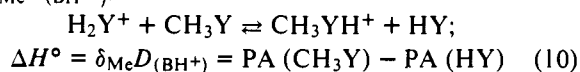
$$\delta_{\text{Me}}D_{(\text{B}^+\text{H})} = \delta_{\text{Me}}D_{(\text{BH}^+)} - \delta_{\text{Me}}\text{IP}_{(\text{B})} \quad (8)$$

$$\delta_{\text{Me}}D_{(\text{BH}^+\text{H}^-)} = \delta_{\text{Me}}\Delta H_{(\text{H}_2)} - \delta_{\text{Me}}D_{(\text{BH}^+)} \quad (9)$$

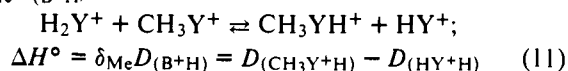
In Table XIII are given the heterolytic and homolytic bond dissociation energies, *D*_(BH⁺) and *D*_(B⁺H), respectively, obtained from eq 4 and 7 and the methyl substituent effects on both for successive replacements of H by methyl substituents in *n*-bases. It is clear from the results in Table XIII that while methyl substituents both stabilize BH⁺ relative to B, and B⁺ relative to BH⁺, there is no quantitative relationship between these two kinds of stabilizing effects. Corresponding values of δ_{Me}*D*_(BH⁺) and -δ_{Me}*D*_(B⁺H) vary from approximately equal to one (either) in great excess of the other.

The greatly divergent methyl stabilizing effects indeed are expected and can be understood in terms of the "reaction processes" involved:¹⁶

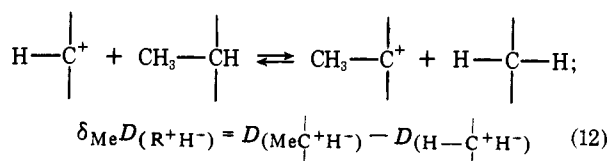
For δ_{Me}*D*_(BH⁺):



For δ_{Me}*D*_(B⁺H):



For δ_{Me}*D*_(R⁺H⁻):

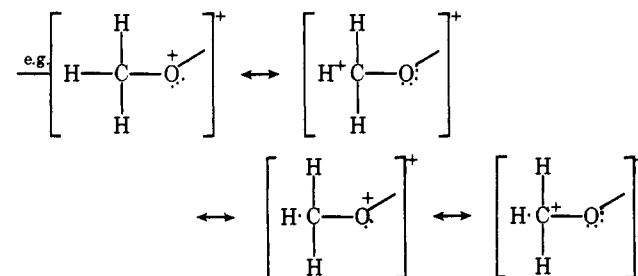


The methyl substituent interactions occur by three principal mechanisms: methyl polarizability (ion-induced dipole interaction) in BH⁺ or B⁺, differential electron transfer through C-Y σ bonds in BH⁺ or B⁺ compared to B (internal inductive effect), and differential stabilization between B⁺ and B resulting from hyperconjugative pseudo π-electron transfer from the CH₃ substituent. The methyl polarizability effect⁵⁵ on reactions 10 and 12 is of major consequence because of the transfer of positive charge to the methyl derivative (CH₃YH⁺)

or CH₃C⁺. This effect is of relatively little consequence in reaction 11 since all species are univalent cations.⁶² Methyl hyperconjugative interaction will predominate in cations (e.g., CH₃C⁺ or CH₃Y⁺) compared to neutral molecules, but it will be small or negligible in formally saturated cations. The internal methyl inductive effect on reactions 10 and 12 will be most important when the reaction is accompanied by a substantial hybridization change.^{59b}

It will be noted (Table XIII) that there are substantially larger methyl substituent effects on proton affinity for phosphorus than for nitrogen *n*-bases, and generally also for sulfur compared to oxygen *n*-bases. The oxygen and nitrogen *n*-bases probably involve predominantly polarizability effects in reaction 10 since formally saturated ions are involved and since hybridization change is small for proton transfer between such bases. The methyl substituent polarizability effects for sulfur and phosphorus *n*-bases are expected to be less than for corresponding polarizability effects for oxygen and nitrogen *n*-bases because of the increased univalent cation radii involved with the former.⁶³ However, this reduced polarizability effect is evidently more than offset by internal inductive effects (P and S *n*-bases involved hybridization changes from ~p³ or p² to sp³ on protonation), and by the hyperconjugative interactions in phosphonium and sulfonium ions involving the interactive d orbitals.⁵⁹ The relative importance of these two effects has yet to be evaluated.

The methyl substituent effects on reaction 11, i.e., -δ_{Me}*D*_(B⁺H) values, may be attributed largely to hyperconjugative effects since the other two methyl substituent effects are small for this H atom transfer reactions between univalent cations.^{59,60,62} This conclusion is supported by the effects of successive methyl substitutions shown in Table XIII. Values



of -δ_{Me}*D*_(B⁺H) are reduced by a factor of 2 for the second methyl substituent compared with the first one—for all four of the onium ion systems. This is the result expected for a substantial delocalization of positive charge into the first methyl substituent thus reducing the charge center with which

Table XIV. Methyl Substituent Effects on Hydride Affinities of Substituted Methyl Cations (kcal mol⁻¹)

	$D_{(R+H^-)}$	$\delta_{Me}D_{(R+H^-)}$
CH ₃ ⁺	313. ⁶⁵	
CH ₃ CH ₂ ⁺	272.5	41.
(CH ₃) ₂ CH ⁺	249.7	22.8
CH ₃ CH ₂ ⁺	272.5	
CH ₃ CHMe ⁺	249.7	22.8
CH ₃ CMe ₂ ⁺	234.8	14.9
HOCH ₂ ⁺	247.8	
HOCHMe ⁺	231.9	15.9
HOCCMe ₂ ⁺	219.5	12.4
C ₆ H ₅ CH ₂ ⁺	239. ⁶⁶	
C ₆ H ₅ CHMe ⁺	229.2	10.
C ₆ H ₅ CMe ₂ ⁺	221.3	7.9

the second methyl substituent interacts. The effects of the third methyl substituents in both N and P cation radicals are indeed small, reduced to about 1/5 of the effect of the first methyl substituent. A quantitative pattern for the effects of successive substitutions on $-\delta_{Me}D_{(B+H)}$ values prevails: 1.00:0.50:0.22. No such magnitude of reduction factors (nor a fixed quantitative pattern) holds for the presumably more composite effects of successive methyl substitution on $-\delta_{Me}D_{(BH^+)}$ values. For example, for ammonium ions, the factors for effects of successive methyl substituent effects on proton affinity are 1:0.73:0.47, whereas for phosphonium ions, they are 1:0.85:0.66.

The methyl substituent effect ($-\delta_{Me}D_{(B+H)}$ values) for lowering of the homolytic bond dissociation energies increase markedly in the sequence P⁺ < S⁺ < N⁺ < O⁺ with the following essentially fixed ratio for corresponding numbers of methyl substitutions: 1.0 (P⁺):2.2 (S⁺):3.8 (N⁺):5.2 (O⁺). In contrast, the largest factor for a corresponding number of methyl substitutions for $\delta_{Me}D_{(BH^+)}$ values is only 2.3 (for the third methyl substitution in phosphonium ions compared to ammonium ions).

The elemental sequence of increased methyl hyperconjugative stabilization of cation radicals need not necessarily be the same as the above elemental sequence of $-\delta_{Me}D_{(B+H)}$ values, i.e., P⁺ < S⁺ < N⁺ < O⁺. This conclusion follows from the fact that reaction 11 gives the *differential* in methyl hyperconjugative stabilization between cation radical and the corresponding onium ion. As noted, only oxonium and ammonium BH⁺s are formally saturated and therefore presumably involve little methyl hyperconjugative stabilization. Thus $-\delta_{Me}D_{(B+H)}$ values for oxonium and ammonium ions give approximately the magnitude of the methyl hyperconjugative stabilizations for these cation radicals. The substantially larger effects of the former may be attributed to increased electron demand (associated with the greater electronegativity of oxygen than nitrogen) in the oxygen cation radical. On the other hand, since sulfonium and phosphonium ion BH⁺s also may be stabilized by methyl hyperconjugative interactions, $-\delta_{CH_3}D_{(B+H)}$ values measure only the (smaller) differentials between the hyperconjugative stabilizations of these ions and their corresponding cation radicals. There is substantial evidence of larger $\pi(p-d)$ conjugative interactions in phosphonium than in corresponding sulfonium ions.⁶⁴ If the methyl hyperconjugative stabilizations follow this sequence, this consideration together with the effect of greater "electron demand" from the S⁺ center of the cation radical may account for the differential methyl hyperconjugative effects of reaction 11 being in the order S⁺ > P⁺.

The above discussion also applies qualitatively to the effects of other alkyl groups. The effects of fluoroalkyl substituents on values of $D_{(B+H)}$ for ammonium ions have been discussed and offer additional evidence for the conclusion that reaction

11 involves largely alkyl substituent hyperconjugative effects.⁶⁰

Table XIV gives methyl substituent effects on the hydride affinities $\delta_{Me}D_{(R+H^-)}$ of methyl cation and substituted methyl cations. The values given for CH₃⁺ and C₆H₅CH₂⁺ are based upon literature values; other values are from Table XI and eq 9.

The largest value of $\delta_{Me}D_{(R+H^-)}$ is for the first methyl substitution in the methyl cation, 41 kcal. This figure greatly exceeds the largest methyl substituent effect observed in Table XIII for any $-\delta_{Me}D_{(B+H)}$ value (CH₃OH⁺). This result is in accord with the nature of eq 12, which, in contrast to either eq 10 or 11, indicates that all three mechanisms of cation stabilization by a methyl substituent are expected to be involved. This conclusion is further supported by the effects of successive methyl substitution on $\delta_{Me}D_{(R+H^-)}$ values. The reduction factors for departure from additivity are not constant between the several series of Table XIV as is observed for the $-\delta_{Me}D_{(B+H)}$ values of Table XIII, and the former factors are intermediate between the latter and those for the effects of successive substitution on proton affinities ($\delta_{Me}D_{(BH^+)}$ values). Further detailed analysis of methyl and other alkyl substituent effects on hydride affinities of carbocations is under continuing study.

The introduction of substituents, e.g., CH₃, OH, or C₆H₅, which increasingly stabilizes the methyl cation⁶⁷ leads to substantial reductions in the magnitude of the methyl substituent effects (Table XIV). The reduction factor tends to be greater the larger the stabilizing effect, i.e., $\delta_{Me}D_{(R+H^-)}$ vs. $D_{(R+H^-)}$ is approximately linear (a relationship analogous to that of Figure 6). This matter is also the subject of continuing study.

Polar Electronegative Substituent Effects and Lone Pair Interactions. Substitution of fluorine for hydrogen both at nitrogen and in methyl or ethyl groups of aliphatic amines leads to marked decreases in proton affinity.^{16,60} Similar effects are found for fluorine substitution in alcohols and esters (cf. Table V). The effects on PA of other polar (positive charge repelling) substituent groups are further revealed by the present results. Thus, substituents Cl and CN, replacing a hydrogen of acetonitrile, reduce proton affinity by 6.1 and 9.3 kcal, respectively. Similarly, substituents CF₃ and CN, replacing the formyl hydrogen of ethyl formate, reduce proton affinity by 8.9 and 10.3 kcal, respectively.

Polar substituent effects are currently under further study. We note at present that the effects on PA of alkyl substituents and of polar substituents for a given functional group are separately correlated by σ_1 polar substituent parameters,⁶⁸ with a slope which is distinctly greater for the former class of substituent than for the latter class. Understanding of this empirical behavior is the subject of subsequent publications.

Aliphatic acyclic and cyclic ethers deserve comment here. In Table XV are given values of IP_(B) (first adiabatic ionization potential), PA(=D_(BH⁺)), and D_(B+H) for these conjugate acids. The proton affinity of 1,4-dioxane is 6.2 kcal less than that of THP. This result provides another example of the base-weakening polar effect of an electronegative substituent, i.e., the ring O atom. The proton affinity of THF is 1.0 kcal less than that of diethyl ether. Since there are the same number of carbon atoms and the two additional slightly polarizable hydrogen atoms of the latter are at large distances, this result may be interpreted to be an internal inductive effect arising within the cyclic ring of THFH⁺. This result is of interest since solution results generally indicate THF to be a stronger base than Et₂O⁶⁹ and also a better hydrogen bond acceptor.⁷⁰ The present results indicate therefore that there are steric effects which weaken both the solvation of Et₂OH⁺ and the hydrogen-bond acceptor ability of Et₂O.

Special stabilization is afforded the radical cations of *n*-

Table XV. Heterolytic and Homolytic Bond Dissociation Energies for the Conjugate Acids of Aliphatic Acyclic and Cyclic Ethers (kcal mol⁻¹)

	IP _(B) ⁴⁴	PA = D _(BH⁺)	D _(B⁺-H)
Dimethyl ether	230.6	190.1	107.1
Diethyl ether	221.6	197.4	105.4
THF	217.2	196.4	100.0
THP	213.3	197.1	96.8
1,4-Dioxane	210.5	190.9	87.8

donor bases that possess several lone pairs which may interact through space or through bonds.⁷¹ This manifests itself in a lowering of the homolytic bond dissociation energy, $D_{(B+H)}$, in comparison to model compounds where such interactions are absent. This has been discussed for the nitrogen compounds CH₂(CN)₂⁵⁰, *trans*-azomethane,⁷² hydrazine,⁷² and diaza-bicyclooctane.⁷³ The data in Table XV afford via eq 4 another example of this phenomenon involving oxygen bases.

Homolytic bond energies of aliphatic acyclic ethers are typically 106 kcal/mol and somewhat lower (~98 kcal/mol) in cyclic ethers. Compared to THP as a model compound, however, it is significant that $D_{(B+H)}$ for 1,4-dioxane is 9.0 kcal mol⁻¹ lower. This can be attributed to lone pair interactions which cause the two resonance structures



to substantially stabilize the radical cation of 1,4-dioxane. Turner has assigned the photoelectron spectrum of 1,4-dioxane, reporting a lone pair splitting of 1.22 eV.⁷⁴

Acknowledgment. We are pleased to acknowledge the technical services of Ms. Heidi Zierau in the synthesis and purification of many of the compounds utilized in this work.

References and Notes

- (1) (a) This work has been supported in part by grants from the National Science Foundation and the Energy Research and Development Administration (Grant E(04-3)-767-8); (b) IREX Visiting Scholar (UCI), 1975-76; (c) Camille and Henry Dreyfus Teacher-Scholar (California Institute of Technology), 1971-1976.
- (2) J. Sherman, *Chem. Rev.*, **11**, 164 (1932).
- (3) M. A. Haney and J. L. Franklin, *J. Phys. Chem.*, **73**, 4328 (1969).
- (4) R. Yamdagni and P. Kebarle, *J. Am. Chem. Soc.*, **98**, 1320 (1976).
- (5) M. T. Bowers, D. H. Aue, H. M. Webb, and R. T. McIver, Jr., *J. Am. Chem. Soc.*, **93**, 4314 (1971).
- (6) J. L. Beauchamp, R. H. Staley, S. E. Buttrill, Jr., J. F. Wolf, I. Koppel, and R. W. Taft, *J. Am. Chem. Soc.*, to be submitted.
- (7) R. W. Taft, J. F. Wolf, J. L. Beauchamp, G. Scorrano, and E. M. Arnett, *J. Am. Chem. Soc.*, in press.
- (8) R. T. McIver, Jr., *Rev. Sci. Instrum.*, **41**, 555 (1970).
- (9) R. T. McIver, Jr., and A. D. Baranyi, *Int. J. Mass Spectrom. Ion Phys.*, **14**, 449 (1974).
- (10) T. B. McMahon and J. L. Beauchamp, *Rev. Sci. Instrum.*, **43**, 509 (1972).
- (11) T. B. McMahon, R. J. Blint, D. P. Ridge, and J. L. Beauchamp, *J. Am. Chem. Soc.*, **94**, 8934 (1972).
- (12) R. T. McIver, Jr., and J. S. Miller, *J. Am. Chem. Soc.*, in preparation.
- (13) W. G. Henderson, M. Taagepera, D. Holtz, R. T. McIver, Jr., J. L. Beauchamp, and R. W. Taft, *J. Am. Chem. Soc.*, **94**, 4728 (1972).
- (14) R. W. Taft, M. Taagepera, K. D. Summerhays, and J. Mitsky, *J. Am. Chem. Soc.*, **95**, 3811 (1973).
- (15) J. F. Wolf, P. G. Harch, and R. W. Taft, *J. Am. Chem. Soc.*, **97**, 2904 (1975).
- (16) R. W. Taft in "Proton Transfer Reactions", E. F. Caldin and V. Gold, Ed., Chapman and Hall, London, 1975, p 31.
- (17) M. S. B. Munson and F. H. Field, *J. Am. Chem. Soc.*, **87**, 4242 (1965).
- (18) L. W. Sieck, F. P. Abramson, and J. H. Futrell, *J. Chem. Phys.*, **45**, 1655 (1966).
- (19) E. G. Jones and A. G. Harrison, *Can. J. Chem.*, **45**, 3119 (1967).
- (20) A. S. Blair and A. G. Harrison, *Can. J. Chem.*, **51**, 1645 (1973).
- (21) T. Su and M. T. Bowers, *J. Am. Chem. Soc.*, **95**, 7609, 7611 (1973).
- (22) R. S. Hemsworth, J. D. Payzant, H. I. Schiff, and D. K. Bohme, *Chem. Phys. Lett.*, **26**, 417 (1974).
- (23) T. B. McMahon, P. G. Miasek, and J. L. Beauchamp, *Int. J. Mass Spectrom. Ion Phys.*, **21**, 63 (1976).
- (24) T. B. McMahon and J. L. Beauchamp, *J. Phys. Chem.*, **81**, 593 (1977).
- (25) R. T. McIver, Jr., and R. C. Dunbar, *Int. J. Mass Spectrom. Ion Phys.*, **7**, 471 (1971).
- (26) G. H. F. Dierksen, W. P. Kraemer, and B. O. Ross, *Theor. Chim. Acta*, **36**, 249 (1975).

- (27) The marginal oscillator was calibrated using a Q-spoiler; cf. A. L. Warneck, L. R. Anders, and T. E. Sharp, *Rev. Sci. Instrum.*, **45**, 929 (1974).
- (28) F. H. Field, J. L. Franklin, and M. S. B. Munson, *J. Am. Chem. Soc.*, **85**, 3575 (1963).
- (29) J. H. Futrell, T. O. Tiernan, F. P. Abramson, and C. D. Miller, *Rev. Sci. Instrum.*, **39**, 340 (1966).
- (30) B. H. Solka and A. G. Harrison, *Int. J. Mass Spectrom. Ion Phys.*, **17**, 379 (1975).
- (31) T. H. Morton and J. L. Beauchamp, *J. Am. Chem. Soc.*, **94**, 3671 (1972).
- (32) D. H. Aue, H. M. Webb, and M. T. Bowers, *J. Am. Chem. Soc.*, **95**, 2699 (1973); Abstracts, 21st Annual Conference on Mass Spectrometry and Applied Topics, San Francisco, Calif., May 20-25, 1973, p 183.
- (33) R. Yamdagni and P. Kebarle, *J. Am. Chem. Soc.*, **95**, 3504 (1973).
- (34) This figure differs from the $\Delta H^\circ_{600} = 33.0 \pm 1-2$ kcal given in Table V due to application of different symmetry number corrections. We take the correction to be $RT \ln (\sigma_{H_2O}/\sigma_{H_3O^+}) (\sigma_{NH_4}/\sigma_{NH_3}) = RT \ln (24/9)$, rather than $RT \ln (18/24)$ used in ref 4.
- (35) J. L. Beauchamp, *Annu. Rev. Phys. Chem.*, **22**, 527 (1971).
- (36) D. H. McDaniel, private communication.
- (37) W. Moffitt, *Proc. R. Soc. London, Ser. A*, **202**, 548 (1950).
- (38) W. A. Chupka and M. E. Russell, *J. Chem. Phys.*, **49**, 5426 (1967).
- (39) H. P. Weise, *Ber. Bunsenges. Phys. Chem.*, **77**, 578 (1973); H. U. Mittmann, H. P. Weise, A. Ding, and A. Henglein, *Z. Naturforsch. A*, **26**, 1112 (1971); H. P. Weise, H. U. Mittmann, A. Ding, and A. Henglein, *ibid.*, **26**, 1122 (1971); S. Peyerimhoff, *J. Chem. Phys.*, **43**, 998 (1965).
- (40) D. K. Bohme in "Interactions between Ions and Molecules", P. Ausloos, Ed., Plenum Press, New York, N.Y., 1975, p 489.
- (41) M. S. Foster and J. L. Beauchamp, *Inorg. Chem.*, **14**, 1229 (1975).
- (42) C. Polley and M. S. B. Munson, Abstracts, 24th Conference on Mass Spectrometry, San Diego, Calif., May 1976, p 723.
- (43) W. J. Hehre, R. T. McIver, Jr., J. A. Pople, and P. v. R. Schleyer, *J. Am. Chem. Soc.*, **96**, 7162 (1974).
- (44) Photoionization potentials have been taken from J. L. Franklin et al., *Nat. Stand. Ref. Data Ser., Nat. Bur. Stand.*, **26** (1969), and A. W. Potts and W. C. Price, *Proc. R. Soc. London, Ser. A*, **326**, 181 (1972).
- (45) H. Hogeveen, A. F. Bickel, C. W. Hilbers, E. L. Mackor, and C. MacLean, *Recl. Trav. Chim. Pays-Bas*, **86**, 687 (1967).
- (46) A. C. Hopkinson, K. Yates, and I. G. Csizmadia, *J. Chem. Phys.*, **52**, 1784 (1970).
- (47) D. H. Aue, H. M. Webb, and M. T. Bowers, *J. Am. Chem. Soc.*, **98**, 311 (1976).
- (48) D. H. Aue, H. M. Webb, and M. T. Bowers, *J. Am. Chem. Soc.*, **97**, 4137 (1975).
- (49) Studies of proton transfer reactions of CH₂NH₂⁺ with NH₃ and ethers indicate that PAs of CH₂=NH and NH₃ are approximately the same: unpublished results of W. T. Huntress and J. L. Beauchamp.
- (50) R. H. Staley, J. E. Kleckner, and J. L. Beauchamp, *J. Am. Chem. Soc.*, **98**, 2081 (1976).
- (51) Unpublished results of Dr. J. L. Abboud.
- (52) G. A. Olah, D. H. O'Brien, and M. White, *J. Am. Chem. Soc.*, **89**, 5694 (1967).
- (53) C. V. Pesheck and S. E. Buttrill, Jr., *J. Am. Chem. Soc.*, **96**, 6027 (1974).
- (54) T. X. Carroll, S. R. Smith, and T. D. Thomas, *J. Am. Chem. Soc.*, **97**, 659 (1975).
- (55) J. I. Brauman and L. K. Blair, *J. Am. Chem. Soc.*, **90**, 5636, 6501 (1968).
- (56) For a recent review cf. J. L. Jensen, *Prog. Phys. Org. Chem.*, **12**, 189 (1976).
- (57) R. W. Taft and M. M. Kreevoy, *J. Am. Chem. Soc.*, **79**, 4011 (1957).
- (58) For evidence of preferential O-protonation of amides in acid solutions, cf. (a) G. Fraenkel, A. Loewenstein, and S. Meiboom, *J. Phys. Chem.*, **65**, 700 (1961); (b) R. J. Gillespie and T. Birchall, *Can. J. Chem.*, **41**, 148 (1963); (c) A. J. Kresge, P. H. Fitzgerald, and Y. Chiang, *J. Am. Chem. Soc.*, **96**, 4698 (1974); (d) R. A. McClelland and W. F. Reynolds, *J. Chem. Commun.*, 824 (1974).
- (59) (a) D. H. McDaniel, N. B. Coffman, and J. M. Strong, *J. Am. Chem. Soc.*, **92**, 6697 (1970); (b) R. H. Staley and J. L. Beauchamp, *ibid.*, **96**, 6252 (1974).
- (60) R. H. Staley, M. Taagepera, W. G. Henderson, I. Koppel, J. L. Beauchamp, and R. W. Taft, *J. Am. Chem. Soc.*, **99**, 326 (1977).
- (61) R. V. Hodges and J. L. Beauchamp, *Inorg. Chem.*, **14**, 2887 (1975).
- (62) W. G. Henderson, M. Taagepera, D. Holtz, R. T. McIver, Jr., J. L. Beauchamp, and R. W. Taft, *J. Am. Chem. Soc.*, **94**, 4728 (1972).
- (63) L. Pauling, "Nature of the Chemical Bond", Cornell University Press, Ithaca, N.Y., 1960, p 514.
- (64) Cf. W. A. Sheppard and R. W. Taft, *J. Am. Chem. Soc.*, **94**, 1919 (1972), and references cited therein.
- (65) K. W. Egger and A. T. Cocks, *Helv. Chim. Acta*, **56**, 1516, 1537 (1973).
- (66) J. M. Abboud, W. J. Hehre, and R. W. Taft, *J. Am. Chem. Soc.*, **98**, 6072 (1976).
- (67) R. W. Taft, R. H. Martin, and F. W. Lampe, *J. Am. Chem. Soc.*, **87**, 2490 (1965).
- (68) Cf. S. Ehrenson, R. T. C. Brownlee, and R. W. Taft, *Prog. Phys. Org. Chem.*, **10**, 1 (1973).
- (69) R. W. Taft, D. Gurka, L. Joris, P. v. R. Schleyer, and J. W. Rakshys, *J. Am. Chem. Soc.*, **91**, 4801 (1969).
- (70) E. M. Arnett, *Prog. Phys. Org. Chem.*, **1**, 223 (1963).
- (71) R. Hoffmann, *Acc. Chem. Res.*, **4**, 1 (1971).
- (72) M. S. Foster, A. D. Williamson, and J. L. Beauchamp, *Int. J. Mass Spectrom. Ion Phys.*, **7**, 471 (1971).
- (73) R. H. Staley and J. L. Beauchamp, *J. Am. Chem. Soc.*, **96**, 1604 (1974).
- (74) J. Daintith, J. P. Maier, D. A. Sweigart, and D. W. Turner, in "Electron Spectroscopy", D. A. Shirley, Ed., North-Holland Publishing Co., Amsterdam, 1972, p 289.